Bends in Optical Dielectric Guides

By E. A. J. MARCATILI

(Manuscript received March 3, 1969)

Light transmission through a curved dielectric rod of rectangular cross section embedded in different dielectrics is analyzed in closed, though approximate form. We distinguish three ranges:

(*i*) *Small cross section guides such as a thin glass ribbon surrounded by air—Making its width 1 percent of the wavelength, most of the power travels outside of the glass; the attenuation coefficient of the guide is two orders of magnitude smaller than that of glass, and the radius of curvature that doubles the straight guide loss is around 10,000*λ.

(*ii*) *Medium cross section guide for integration optics—It is only a few microns on the side and capable of guiding a single mode either in low loss bends with short radii of curvature or in a high Q closed loop useful for filters. Q's of the order of* 10^8 *are theoretically achievable in loops with radii ranging from 0.04 to 1 mm, if the percentage refractive index difference between guide and surrounding dielectric lies between 0.1 and 0.01.*

(*iii*) *Large cross section guides—They are multimode and are used in fiber optics. Conversion to higher order modes are found more significant than radiation loss resulting from curvature.*

I. INTRODUCTION

A dielectric rod, embedded in one or more dielectrics of lower refractive index, is the basic ingredient of three types of optical waveguide which differ only in their relative dimensions and consequently in their guiding properties.

The first is a small cross section guide which supports only the fundamental mode; most of the power travels in a lower loss external medium. Thus, the attenuation of the mode is smaller than if all the power flowed through the higher loss internal medium. Tiny rods, thin ribbons, or films made of glass or other substances embedded in either air or low loss liquids are typical examples.[1-3]

The second is a medium size guide capable of supporting only a few

modes; most of the power travels in the internal medium. Such a guide, (Fig. 1 of Ref. 10) has been proposed as the building block of passive and active components for integrated optical circuitry.[4-6] Lasers, modulators, directional couplers, and filters are some of the many devices which could be built in a single substrate utilizing the high precision techniques available from integrated circuitry; consequently they would be compact, mechanically stable, and reproducible.

The third, a large size guide (clad fiber) which can support many modes, is used typically in fiber optics.[7]

These basic guides, having round or rectangular cross section and straight axis, have been studied both analytically and through computer calculations.[8-13] Also the directional coupler (Fig. 2 of Ref. 10) obtained by running two guides of rectangular or circular cross sections parallel to each other, has been analyzed.[10,12,14]

To my knowledge, though, little is known quantitatively about the ability of any of the three types of guides to negotiate bends, or about the radiation losses in loops, such as the one depicted in Fig. 1 as part of a channel dropping filter. This paper should supply such information.

In Section II the boundary value problem is discussed, and the fundamental modes of each polarization are described. Section III contains a discussion of the results and numerical examples. Conclusions are drawn in Section IV and all the mathematical derivations are exiled to the appendix.

II. FORMULATION OF THE BOUNDARY VALUE PROBLEM

Figure 2 depicts, in perspective, the basic geometry of the curved guide with radius of curvature R. The cross section is a rectangle whose sides are a and b. The refractive index of the guide is n_1, and the refractive indices around the guide are n_2, n_3, n_4, and n_5, all of which are smaller than n_1. Furthermore, for reasons which become apparent later, we do not specify the refractive indices in the four shaded areas.

This boundary value problem is solved in closed, though approximate form in the appendix, by introducing the same simplification used in solving the problem of transmission in the straight guide.[10] That simplification arises from solving Maxwell's equations only for guide dimensions such that a small percentage of the total power flows through the shaded areas and consequently a negligible error is expected if one does not match properly the fields along their edges.

Two types of hybrid modes propagate through this curved guide;

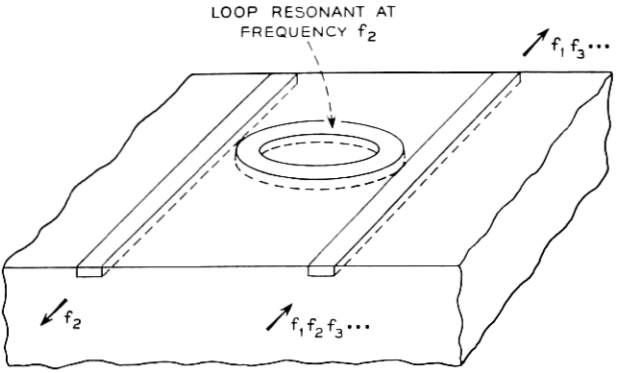

Fig. 1 — Channel dropping filter (ring type).

each one has six field components. But since some of the refractive indices n_2, n_3, n_4, and n_5 are chosen close to n_1, guidance occurs through total internal reflection only when the plane wavelets that make a mode impinge on the interfaces at grazing angles. Consequently, the only large field components are perpendicular to the curved z axis (Fig. 2). The modes are then of the TEM kind and we group them in two families, E^x_{pq} and E^y_{pq}. The main field components of the members of the first family are E_x and H_y, while those of the second are E_y and H_x.

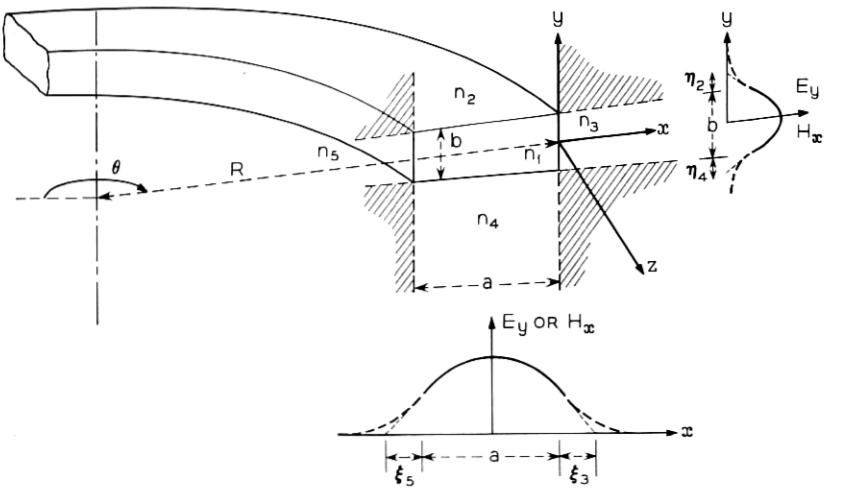

Fig. 2 — Curved dielectric guide.

Virtually every one of these components varies sinusoidally along x and y within the guiding medium 1 and decays exponentially in the surrounding media 2, 3, 4, and 5 (Fig. 2). The subindices p and q represent the number of extrema of each field component in the x and y directions, respectively. The field configurations of some members of the two families in straight guides are depicted in Fig. 5 of Ref. 10; section 2.1 describes the influence of a finite radius of curvature on those field configurations.

General expressions for the different phase and propagation constants in each medium of the curved guide are calculated in the appendix, for arbitrary modes and for $n_2 \neq n_3 \neq n_4 \neq n_5$. In the text, we consider only the fundamental modes of each family E^x_{11} and E^y_{11}; furthermore, we choose

$$n_3 = n_5 \tag{1}$$

and leave n_2 and n_4 arbitrary. This choice of refractive indexes encompasses the most interesting cases.

2.1 E^x_{11} Mode

We first study the E^x_{11} mode. As we said before, the main components are E_x along the x direction and H_y along y. Both components have a single maximum located within medium 1 and drop sinusoidally toward the edge of it. Outside of the medium, the decay is exponential.

The axial propagation constant is according to equation (47)

$$k_z = (k_1^2 - k_x^2 - k_y^2)^{\frac{1}{2}}, \tag{2}$$

where $k_1 = kn_1 = (2\pi/\lambda)n_1$ and λ is the free space wavelength, k_x is the propagation constant along x in media 1, 2, and 4, and k_y is the propagation constant along y in media 1, 3, and 5. This means that the electrical width of media 1, 2, and 4 is the same and equal to $k_x a$, and the electrical height of 1, 3, and 5 is also the same and equal $k_y b$.

The transverse propagation constant k_y is independent of the radius of curvature R and can be found from the transcendental equation (37)

$$k_y b = \pi - \tan^{-1}\left[\left(\frac{\pi}{k_y A_2}\right)^2 - 1\right]^{-\frac{1}{2}} - \tan^{-1}\left[\left(\frac{\pi}{k_y A_4}\right)^2 - 1\right]^{-\frac{1}{2}} \tag{3}$$

in which

$$A_{\substack{2\\4}} = \frac{\lambda}{2\left(n_1^2 - n_{\substack{2\\4}}^2\right)^{\frac{1}{2}}}. \tag{4}$$

If the height of the guide b is selected so large that

$$\frac{A_2 + A_4}{\pi b} \ll 1, \tag{5}$$

only a small percentage of the power carried by the mode travels in media 2 and 4; and equation (3) can be solved approximately, yielding

$$k_y = \frac{\pi}{b}\left(1 + \frac{A_2 + A_4}{\pi b}\right)^{-1}.$$

According to equation (49), the other transverse propagation constant

$$k_x = k_{x0}\left[1 + \frac{2c}{ak_{x0}} - i\frac{k_{x0}\alpha_c}{k_{x0}^2}\right] \tag{6}$$

is valid if

$$\begin{aligned} \frac{c}{ak_{x0}} &\ll 1 \\ \alpha_c R &\ll 1. \end{aligned} \tag{7}$$

The first term in equation (6), k_{x0}, is the propagation constant in the x direction of the guide without curvature; the second and third terms, which according to equation (7) must be small, are perturbations related to the change of field profile and to radiation loss, both of which are introduced by the curvature. More precisely, α_c is the attenuation coefficient of the curved guide, $\alpha_c R$ is the attenuation per radian, that is the attenuation in a length of guide equal to R, and c is a conversion loss coefficient such that, at a junction between a straight and a curved section of the same guide, c^2 measures the power that the fundamental mode in the straight section would couple to modes higher than the fundamental in the curved section. The fact that equation (6) is valid if $c \ll 1$ requires the radius of curvature R to be so large that the field profiles of the fundamental modes in the straight and curved guides are quite similar. Later in this section we consider formulas applicable when $c \cong 1$.

The axial propagation constant, k_{z0}, of the straight guide is related to k_{x0} and k_y by the expression

$$k_{z0} = (k_1^2 - k_{x0}^2 - k_y^2)^{\frac{1}{2}}; \tag{8}$$

and k_{x0} is the solution of the transcendental equation (55)

$$k_{x0}a = \pi - 2\tan^{-1}\frac{n_3^2}{n_1^2}\left[\left(\frac{\pi}{k_{x0}A}\right)^2 - 1\right]^{-\frac{1}{2}}. \tag{9}$$

The length

$$A = \frac{\lambda}{2(n_1^2 - n_3^2)^{\frac{1}{2}}} \tag{10}$$

is used as a normalizing dimension. What does it measure? If one assumes $b = \infty$, the guide becomes a slab of width a. If $a \leqq A$, only the fundamental mode is guided; if $a > A$, the slab is multimode.

Figure 3 is a graph of the electrical width, $k_{x0}a$, of the straight guide as a function of a/A. The solid curve is the solution of equation (9) assuming $n_1/n_3 = 1.5$, while the dotted one is the solution for $n_1/n_3 = 1$. For thin guides, $a/A \ll 1$, the electrical width is proportional to a; for thick guides, $a/A \gg 1$, the electrical width goes asymptotically to π.

The attenuation per radian $\alpha_c R$ and the conversion coefficient c, obtained from equations (50) and (51) with $n_3 = n_5$ are

$$\alpha_c R = \frac{1}{2}\left(1 - \frac{n_3^2}{n_1^2}\right)^{-\frac{1}{2}}\left(\frac{n_3 k_{x0}a}{n_1}\right)^2\left(\frac{A}{\pi a}\right)^3\left[1 - \left(\frac{k_{x0}A}{\pi}\right)^2\right]^{\frac{1}{2}} \cdot \frac{\mathfrak{R}\exp\left\{-\frac{\mathfrak{R}}{3}\left[1 - \left(\frac{k_{x0}A}{\pi}\right)^2\left(1 + \frac{2c}{ak_{x0}}\right)^2\right]^{\frac{3}{2}}\right\}}{1 - \left(1 - \frac{n_3^4}{n_1^4}\right)\left(\frac{k_{x0}A}{\pi}\right)^2 + 2\frac{n_3^2 A}{n_1^2 a}\left[1 - \left(\frac{k_{x0}A}{\pi}\right)^2\right]^{-\frac{1}{2}}} \tag{11}$$

and

$$c = \frac{1}{2k_{x0}a}\left(\frac{\pi a}{A}\right)^3\frac{1}{\mathfrak{R}}, \tag{12}$$

where

$$\mathfrak{R} = \frac{2\pi^3 R}{k_{x0}^2 A^3} = 2\frac{k_1^3}{k_{x0}^2}\left(1 - \frac{n_3^2}{n_1^2}\right)^{\frac{3}{2}}R. \tag{13}$$

The solid curves in Figs. 4 and 5 are graphs of the function

$$\alpha_c R\left(1 - \frac{n_3^2}{n_1^2}\right)^{\frac{1}{2}}$$

(which is proportional to the attenuation per radian) as a function of a/A using $\mathfrak{R}$ as a parameter. In Fig. 4, we further assume that

$$\frac{n_1}{n_3} = 1 + \Delta$$

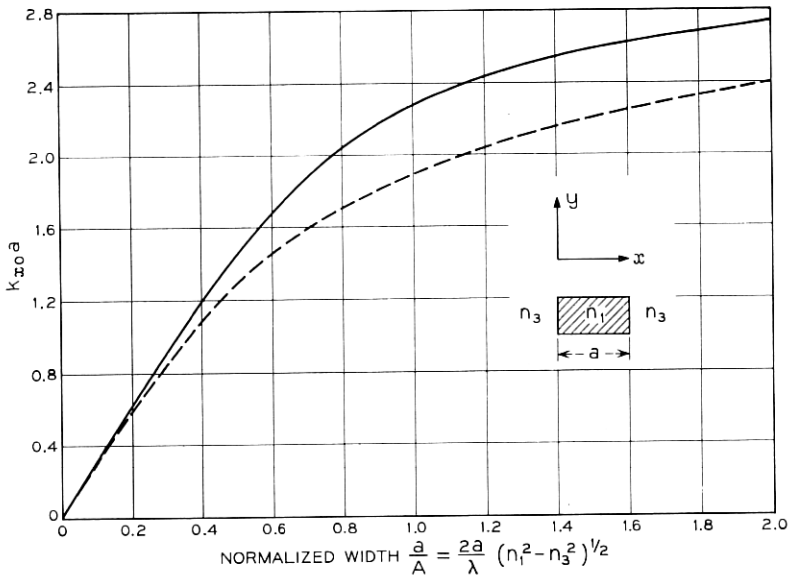

Fig. 3—Guide's electrical width. Solid line is for E_{11}^z mode with $n_1/n_3 = 1.5$; dashed line is for E_{11}^z mode with n_1/n_3 arbitrary, and for E_{11}^x mode with $n_1 \cong n_3$.

and

$$\Delta \ll 1;$$

in Fig. 5,

$$\frac{n_1}{n_3} = 1.5.$$

In the same figures each dashed line is a curve of constant conversion loss c. Since the calculations are valid for $c \ll 1$, we believe the solid curves are reliable to the left of the dotted curve $c = 0.3$ and grow progressively in error to the right of it.

To extend the use of this graph to arbitrarily large values of a/A, we calculate the loss per radian, equation (63), when $a/A \gg 1$ and $c \cong 1$. It is

$$\alpha_c R = \frac{n_3^2}{n_1^2}\left[1 - \left(\frac{n_3}{n_1}\right)^2\right]^{-\frac{1}{2}} \exp\left\{-\frac{\Re}{3}\left[1 - \left(\frac{9\pi}{2\Re}\right)^{\frac{2}{3}} + \frac{4n_3^2}{n_1^2\Re}\right]^{\frac{3}{2}}\right\}; \qquad (14)$$

the dotted lines in Figs. 4 and 5 represent this loss. The reader can smoothly extend the solid curves to the right of the dashed line, $c = 0.3$, so that they become asymptotic to the dotted lines. Thus, the whole range of guide width a from 0 to R has been covered.

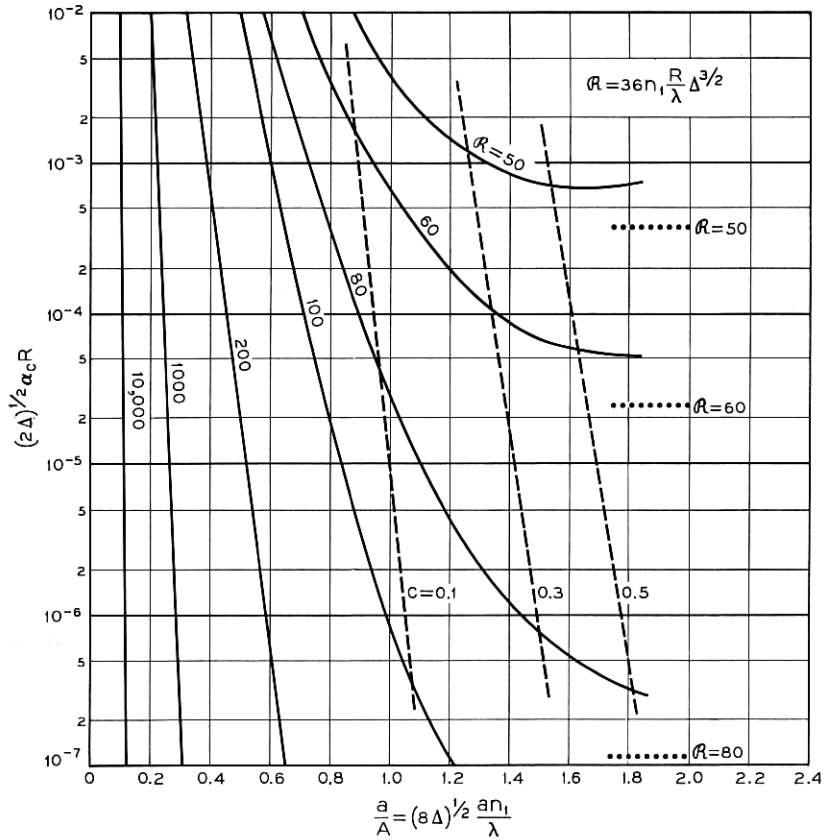

Fig. 4 — Attenuation per radian for E_{11}^x and E_{11}^y modes if $n_1/n_3 = 1 + \Delta$ and $\Delta \ll 1$.

To understand why these curves of constant R become asymptotic for $a/A \gg 1$, we have drawn in Fig. 6a a curved guide with a certain R; its width a is very large compared with A. Also the amplitudes of the field components E_x and H_y are plotted as functions of x and y.

Along x the field inside the guide behaves virtually as the Bessel function $J_\nu[k_1(R + x)]$ where ν is a very large number and outside of the guide decays exponentially. This guide has some radiation loss per radian.

Now, suppose that we start shrinking a without changing R. Since the field at $x = -a$ is very small, the radiation loss remains constant until a is made so short that the field at $x = 0$ and $x = -a$ are com-

parable (Fig. 6b). The field inside the guide varies almost sinusoidally, while outside decays exponentially and the attenuation per radian increases. If a is reduced even further (Fig. 6c) most of the power travels outside of the guide, and the loss increases even more. The field configuration along y is practically the same in the three cases (Fig. 6).

For resonant loops, such as the filter in Fig. 1, the intrinsic Q resulting from curvature radiation is more interesting than the attenuation α_c. They are related by the expression

$$Q_c = \frac{k_{z0}}{2\alpha_c}. \tag{15}$$

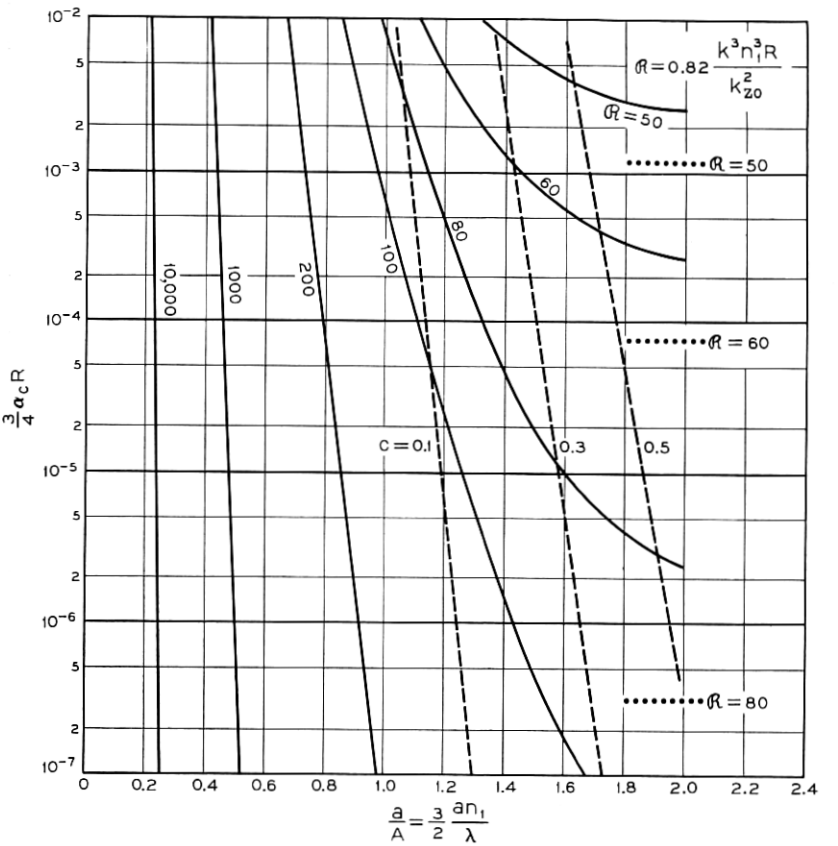

Fig. 5 — Attenuation per radian for E_{11}^x mode if $n_1/n_3 = 1.5$.

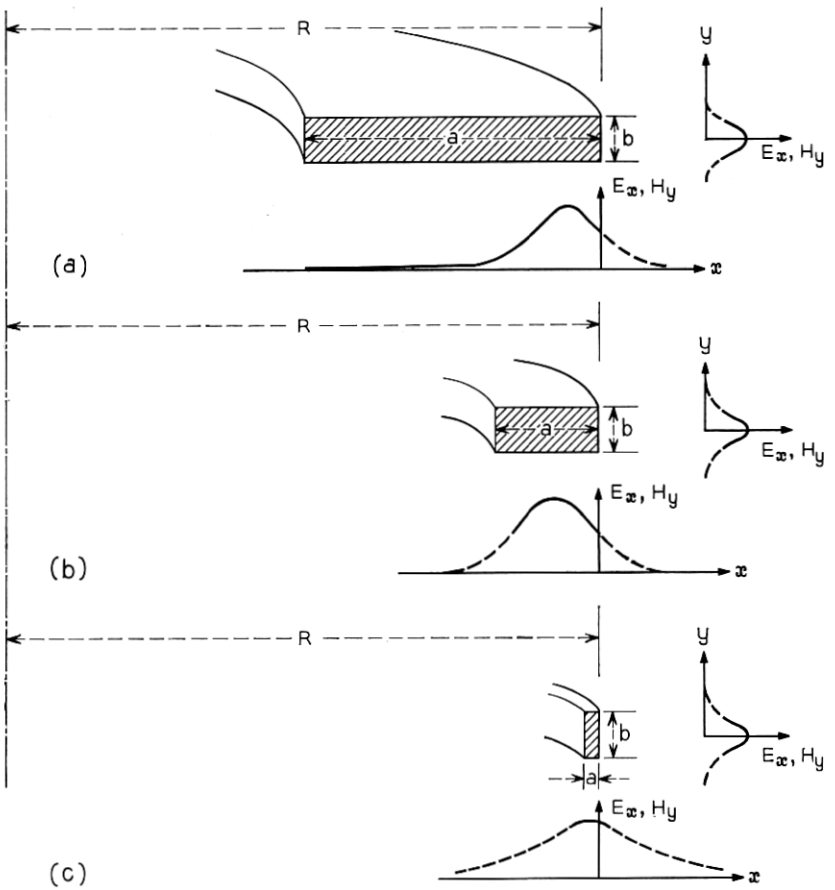

Fig. 6 — Field distribution as a function of guide width a with (a) $a/A \gg 1$, (b) $a/A \cong 1$, and (c) $a/A \ll 1$.

This function is plotted in Fig. 7, assuming

$$\frac{n_1}{n_3} = 1 + \Delta$$

and

$$\Delta \ll 1$$

and in Fig 8, assuming

$$\frac{n_1}{n_3} = 1.5,$$

using as before the normalized guide width a/A as variable and $\mathcal{R}$ as parameter. As in Figs. 4 and 5, the reader can easily match the solid and dotted curves. Further discussion of these curves is reserved for Section III.

The field components in media 2, 3, 4, and 5 decay almost exponentially away from the guiding rod, and the distances η_2, η_4, ξ_3, and ξ_5 over which the fields decrease by $1/e$ are

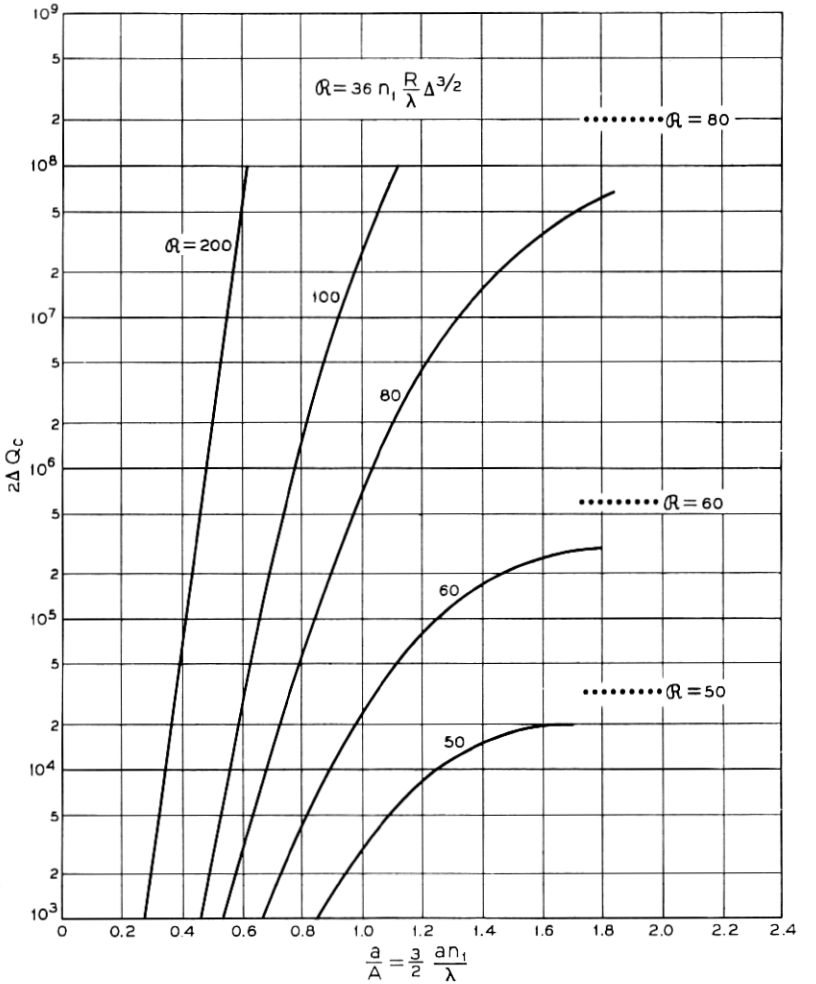

Fig. 7 — Intrinsic Q for $E_{11}{}^x$ and $E_{11}{}^y$ modes if $n_1/n_3 = 1 + \Delta$ and $\Delta \ll 1$.

$$\eta_{\substack{2\\4}} = \frac{1}{|k_{y\substack{2\\4}}|} = \frac{1}{\left(k_1^2 - k_{\substack{2\\4}}^2 - k_y^2\right)^{\frac{1}{2}}}, \tag{16}$$

$$\xi_3 = \xi_5 = \frac{1}{|k_{x3}|} = \frac{1}{(k_1^2 - k_3^2 - |k_x^2|)^{\frac{1}{2}}}. \tag{17}$$

2.2 E_{11}^y Mode

We now consider the E_{11}^y mode. The main components are E_y and H_x; they are qualitatively quite similar to components of the E_{11}^x mode, rotated 90°.

The propagation constant k_z is still given by equation (2); but now k_y

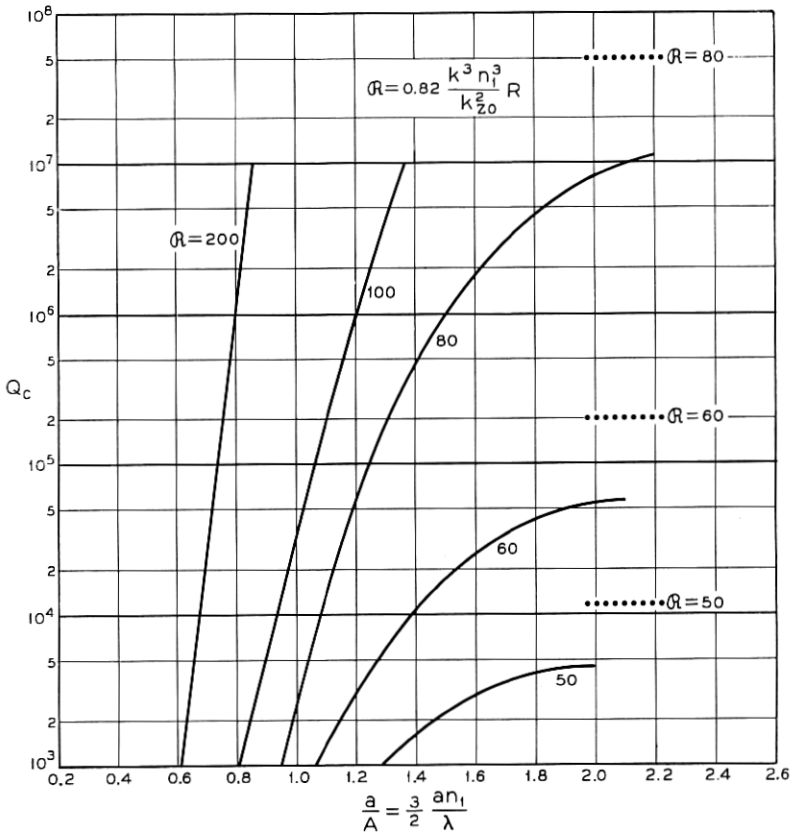

Fig. 8 — Intrinsic Q for E_{11}^x mode if $n_1/n_3 = 1.5$.

is the solution of

$$k_y b = \pi - \tan^{-1} \frac{n_2^2}{n_1^2} \left[\left(\frac{\pi}{k_y A_2} \right)^2 - 1 \right]^{-\frac{1}{2}} - \tan^{-1} \frac{n_4^2}{n_1^2} \left[\left(\frac{\pi}{k_y A_4} \right)^2 - 1 \right]^{-\frac{1}{2}}. \tag{18}$$

The equivalent formula of any of those between equation (7) and (17) can be derived from that formula by substituting the ratio of refractive indexes by unity, but leaving them unchanged wherever they are subtracted from unity. For example, equation (11) becomes

$$\alpha_c R = \frac{1}{2} \left[1 - \left(\frac{n_3}{n_1} \right)^2 \right]^{-\frac{1}{2}} (k_{x0} a)^2 \left(\frac{A}{\pi a} \right)^3 \left[1 - \left(\frac{k_{x0} A}{\pi} \right)^2 \right]^{\frac{1}{2}} \cdot \frac{\Re \exp \left\{ -\frac{\Re}{3} \left[1 - \left(\frac{k_{x0} A}{\pi} \right)^2 \left(1 + \frac{2c}{a k_{x0}} \right)^2 \right]^{\frac{3}{2}} \right\}}{1 - 2\left(1 - \frac{n_3^2}{n_1^2} \right) \left(\frac{k_{x0} A}{\pi} \right)^2 + 2 \frac{A}{a} \left[1 - \left(\frac{k_{x0} A}{\pi} \right)^2 \right]^{-\frac{1}{2}}}, \tag{19}$$

while c and $\Re$ given by equations (12) and (13) remain unchanged.

Figure 9 is a graph of the function $\alpha_c R[1 - (n_3/n_1)^2]^{\frac{1}{2}}$, valid for any ratio n_1/n_3. In particular, for $n_1/n_3 = 1 + \Delta$ and $\Delta \ll 1$, equations (19) and (11) become the same, and consequently these curves coincide with those in Fig. 4. This means that for $n_1 \cong n_3$, the E_{11}^x and E_{11}^y modes have the same loss.

Figure 10 is a graph of the intrinsic Q of a loop operating in the E_{11}^y mode which can be derived from equations (15) and (19). As before, in a resonant loop with $n_1/n_3 = 1 + \Delta$ and $\Delta \ll 1$, the E_{11}^x or E_{11}^y modes have the same Q's.

III. DISCUSSION AND EXAMPLES

The attenuation per radian of any dielectric guide of rectangular cross section and the Q_c resulting from curvature are strongly dependent on the radius of curvature. With the help of equation (17), the attenuation per radian equation (11) can be written

$$\alpha_c R = MR \exp \left(-\frac{1}{6\pi^2} \frac{\lambda_z^2 R}{|\xi_3|^3} \right), \tag{20}$$

where M is independent of R, λ_z is the guided wavelength along z, and ξ_3 is the length over which the field in medium 3 decays by $1/e$. According to Fig. 11, the function

$$R \exp \left(-\frac{1}{6\pi^2} \frac{\lambda_z^2 R}{|\xi_3|^3} \right)$$

becomes negligibly small, and consequently the attenuation per radian becomes negligibly small when

$$R > \frac{24\pi^2 \mid \xi_3 \mid^3}{\lambda_z^2}. \tag{21}$$

This simple criterion is developed further in Ref. 15.

We are interested, though, in a more detailed description of transmission through a bent dielectric guide. Given a guide with a certain radius of curvature (that is, given R and a/A), in general the loss per radian of the E_{11}^x mode is much larger than that of the E_{11}^y mode (compare, for example, Figs. 5 and 9 for $n_1/n_3 = 1.5$). That difference becomes negligible if $n_1/n_3 - 1 \ll 1$.

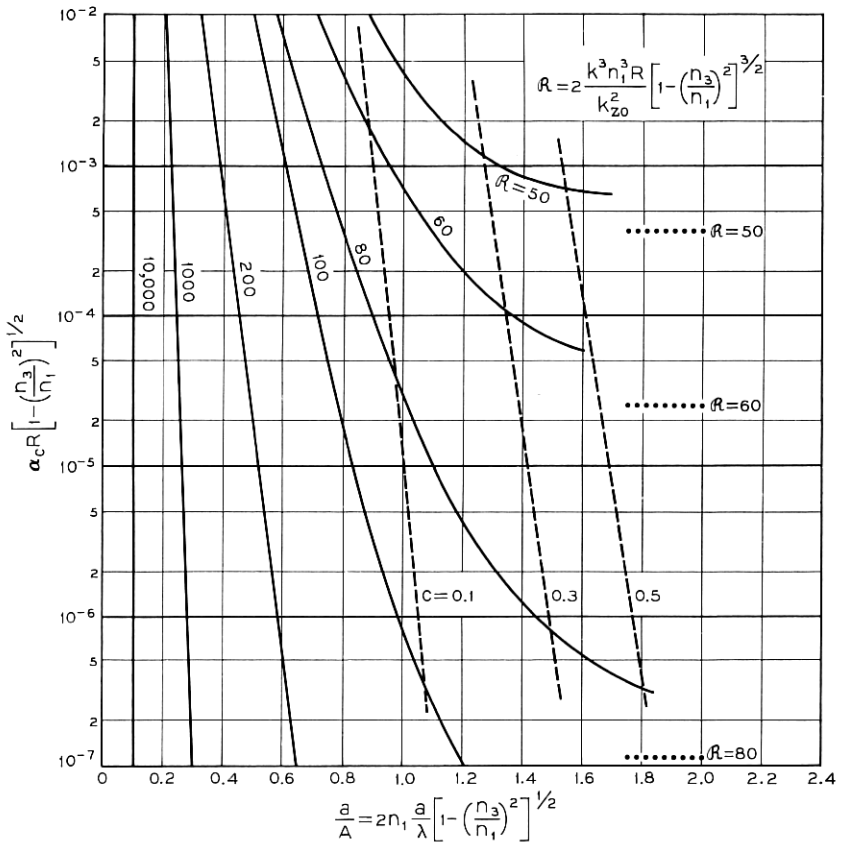

Fig. 9 — Attenuation per radian for E_{11}^y mode and $n_1/n_3 > 1$.

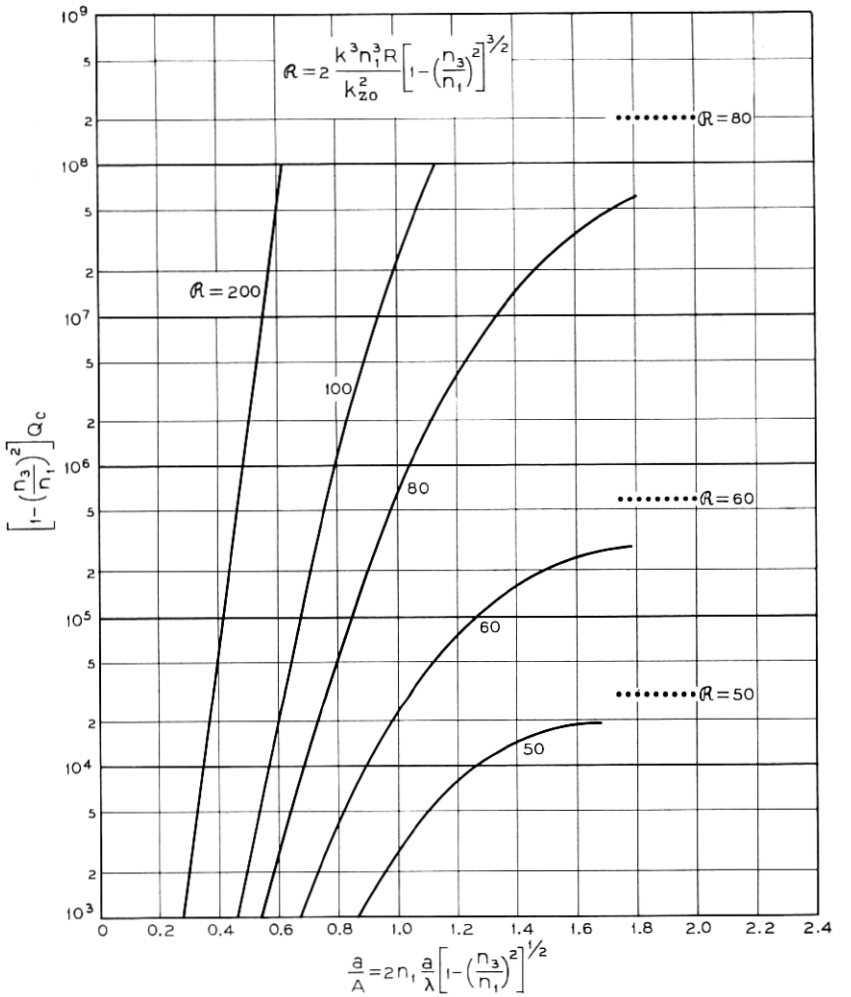

Fig. 10 — Intrinsic Q for $E_{11}{}^y$ mode and $n_1/n_3 > 1$.

Let us consider separately the three types of guide: thin, medium and large.

3.1 *Thin or Low Loss Guides**

In thin guides the width a is so small that

* Low loss for straight guide.

$$\frac{a}{A} = \frac{2a(n_1^2 - n_3^2)^{\frac{1}{2}}}{\lambda} \ll 1. \tag{22}$$

The height b of the guide must be large so that only a little part of the power travels in the shaded areas of Fig. 2. Assuming that the guiding rod dielectric is lossy, its refractive index is

$$n_1 = n\left(1 + \frac{i\alpha}{kn}\right), \tag{23}$$

where n is real and α is the attenuation constant of a plane wave in that medium.

Substituting equations (22) and (23) in equations (2), (11), and (12), we obtain

$$k_z = k_{z0} + i\alpha_s + i\alpha_c . \tag{24}$$

The first term

$$k_{z0} = (k_3^2 - k_y^2)^{\frac{1}{2}} \begin{cases} 1 + \frac{1}{8}\left[k_3 a\left(1 - \frac{n_3^2}{n^2}\right)\right]^2 & \text{for } E_{11}^x \text{ mode} \\ 1 + \frac{1}{8}\left[k_3 a\left(\frac{n^2}{n_3^2} - 1\right)\right]^2 & \text{for } E_{11}^y \text{ mode} \end{cases} \tag{25}$$

is the phase constant. Since most of the power travels in the external medium, its value for either mode is close to kn_3. The conversion loss term c is negligible.

The imaginary part of equation (24) is the attenuation constant, and is made of two terms. The first term

$$\alpha_s = \frac{\alpha}{2} n n_3 k^2 a^2 \left(\frac{n^2}{n_3^2} - 1\right) \begin{cases} \left(\frac{n_3}{n}\right)^6 & \text{for } E_{11}^x \text{ mode} \\ 1 & \text{for } E_{11}^y \text{ mode} \end{cases} \tag{26}$$

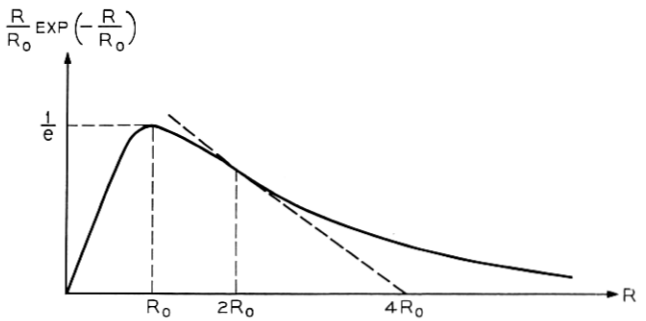

Fig. 11 — Plot of $R/R_0 \exp(-R/R_0)$ and tangent at inflection point.

is the attenuation that each mode would have if the guide were straight.[16] The second term

$$\alpha_c = \frac{k_3^3 a^2}{8}\left(\frac{n^2}{n_3^2}-1\right)^2 \cdot \begin{cases} \left(\frac{n_3}{n}\right)^4 \exp\left\{-\frac{k_3^4 a^3 R}{12}\left(\frac{n_3}{n}\right)^6\left(\frac{n^2}{n_3^2}-1\right)^3\left[1-\frac{1}{2}\left(\frac{k_y}{k_3}\right)^2\right]\right\} & \text{(for } E_{11}^x \text{ mode)} \\ \exp\left\{-\frac{k_3^4 a^3 R}{12}\left(\frac{n^2}{n_3^2}-1\right)^3\left[1-\frac{1}{2}\left(\frac{k_y}{k_3}\right)^2\right]\right\} & \text{(for } E_{11}^y \text{ mode)} \end{cases} \tag{27}$$

is the attenuation resulting from the radiation introduced by the curvature. The E_{11}^y mode is more tightly bound to the guiding rod and consequently has more straight loss and less curvature loss than the E_{11}^x mode.

From equations (26) and (27), the radius of curvature R_d that doubles the straight guide loss is

$$R_d = \frac{12}{k_3}\left[\frac{\alpha n}{2\alpha_s n_3\left(\frac{n^2}{n_3^2}-1\right)}\right]^{\frac{1}{3}}\left[1-\frac{1}{2}\left(\frac{k_y}{k_3}\right)^2\right]^{-1} \cdot \begin{cases} \left(\frac{n_3}{n}\right)^3 \log\left[\frac{kn}{4\alpha}\left(\frac{n^2}{n_3^2}-1\right)\right] & \text{(for } E_{11}^x \text{ mode).} \\ \log\left[\frac{kn_3^2}{4\alpha n}\left(\frac{n^2}{n_3^2}-1\right)\right] & \text{(for } E_{11}^y \text{ mode).} \end{cases} \tag{28}$$

Example 1: Consider a thin ribbon guide made of glass surrounded by air and assume that $n = 1.5$, $n_3 = 1$, $\alpha = 0.1$ nepers per m, and $b = \infty$. From equations (26) and (28) we calculate the values in Table I.

It is doubly advantageous to use the E_{11}^x mode rather than the E_{11}^y because (*i*) the thickness required for equal radiation loss and straight guide loss is roughly $(n/n_3)^3$ times larger, and (*ii*) R_d is about $(n/n_3)^3$ times smaller.

If the height b of the ribbon is finite, k_y/kn_3 is no longer zero and the radii are, according to equation (28), $[1 - \frac{1}{2}(k_y/k_3)^2]^{-1}$ times longer than those in Table I.

3.2 *Medium Size Guide for Integrated Optical Circuitry*

It is likely that guides for integrated optical circuitry will be possible to fabricate only with $n_1 \cong n_3$. The radiation loss per radian and the Q_c of

TABLE I—VALUES CALCULATED FROM EQUATIONS (26) AND (28)

α_s (nepers/m)	E_{11}^y Mode		E_{11}^x Mode	
	$\frac{a}{\lambda}$	$\frac{R_d}{\lambda}$	$\frac{a}{\lambda}$	$\frac{R_d}{\lambda}$
0.01	0.05	1.9×10^3	0.17	6.3×10^2
0.001	0.016	6.2×10^4	0.055	2×10^4
0.0001	0.005	2×10^6	0.017	6.5×10^5

loops made with these guides can be obtained from Figs. 4 and 7, considering abscissas around $a/A = 1$. For both modes, E_{11}^y and E_{11}^x, most of the power travels within the guiding rod.*

In general, the losses are very sensitive to the radius of curvature. They are also sensitive to the guide's width to the left of the dashed curve $c = 0.5$, but fairly insensitive to the right of it.

Example 2: Let us design a guide:

(*i*) The attenuation per radian resulting from radiation loss is

$$\alpha_c R = 0.01 \text{ nepers} = 0.087 \text{ dB}.$$

(*ii*) Its width a is the maximum compatible with single mode guidance in the infinitely high slab, that is

$$\frac{a}{A} = \frac{2a}{\lambda}(n_1^2 - n_3^2)^{\frac{1}{2}} = 1.$$

(*iii*) We assume $b = \infty$ and $n_3 = n_1(1 - \Delta)$, where $\Delta \ll 1$ and $n_1 = 1.5$.

From Fig. 4 we derive the guide dimensions for different values of Δ:

Δ	$\frac{a}{\lambda}$	$\frac{R}{\lambda}$
0.1	0.745	30
0.01	2.36	1,060
0.001	7.45	37,000

Unless Δ is 0.01 or larger, the radius of curvature R becomes uncomfortably large for integrated optical circuitry. Furthermore, if b is finite, k_y is no longer zero, and the radii become $[1 - (k_y/k_3)^2]^{-1}$ times larger than those in the table above.

* This is not true if $b/B_2 \ll 1$. Then k_{z0} must be calculated from equation (8).

Example 3: We design a resonant loop (Fig. 1) such that its Q_c resulting from radiation is equal to the Q resulting from transmission loss in typical glass ($n_1 = 1.5$, $\alpha = 0.1$ neper/m at $\lambda = 1\mu$); that is,

$$Q = Q_c = 5 \times 10^7.$$

Furthermore, let us assume as in Example 2 that $a/A = 1$, $n_3 = n_1(1 - \Delta)$, and $b = \infty$. With the help of Fig. 7 we derive

Δ	$\frac{a}{\lambda}$	$\frac{R}{\lambda}$
0.1	0.745	57
0.01	2.36	1,550
0.001	7.45	42,000

Again, unless Δ is larger than 0.01, the radius of curvature becomes unwieldily large for integrated optical circuitry.

Instead of using a loop as the resonant circuit of Fig. 1, it is possible to make $a = R$, and the loop becomes a pillbox (Fig. 12). This structure may be simpler to fabricate. For this case, also from Fig. 4, using the refractive indices of the previous example, we obtain

Δ	$\frac{R}{\lambda}$
0.1	42
0.01	1,170
0.001	32,000

The pillbox resonator requires a 30 percent shorter radius than the ring resonator. As before, if b is finite, the radii are $[1 - (k_y/k_3)^2]^{-1}$ times longer than those in the last two tables.

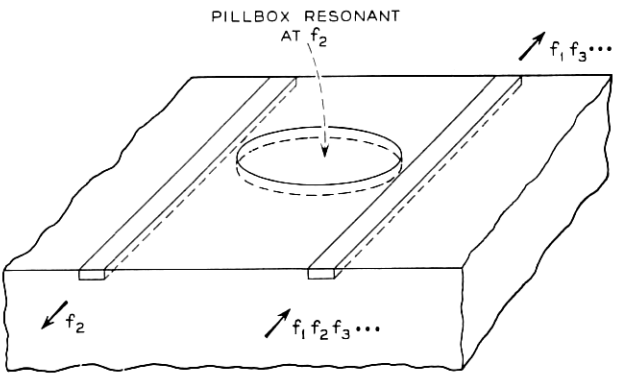

Fig. 12 — Channel dropping filter (pillbox type).

3.3 *Large Guides for Fiber Optics*

The large guide is multimode, $a/A \gg 1$, and the radius for small mode conversion is derived from equations (11) and (12), making $k_{x0}a = \pi$ and $k_{z0} = 2\pi n_1/\lambda$. Then

$$c = \pi n_1^2 \frac{a^3}{\lambda^2 R}.$$

For a power conversion $c^2 = 0.01$, and $n_1 = 1.5$, we have

$\frac{a}{\lambda}$	$\frac{R}{\lambda}$
5	8,900
10	71,000

The conversion loss is many orders of magnitude larger than the loss radiated by the fundamental mode because of the curvature. Radiation loss of higher order modes can be found in equations (51) and (63).

In general, clad fibers are of circular cross section; consequently our calculations do not strictly apply. Nevertheless, a guide of circular cross section and another of equal area but square cross section must have quite comparable attenuation per radian unless mode degeneracy occurs, but this is quite unlikely.

Though we have been talking throughout of light guides, it is obvious that all the calculations are equally applicable to microwave guides.

IV. CONCLUSIONS

Relations between radiation losses resulting from curvature, geometry, and electric characteristics of the bent dielectric guide are summarized in Figs. 4, 5, and 7 through 10 and they are discussed and exemplified in Section III.

The main qualitative results are that for a given radius of curvature R, the radiation loss can be reduced

(*i*) by increasing the difference between the refractive index n_1 of the guide and those of the media toward the outside, n_3, and inside, n_5, of the curved guide axis (Fig. 2);

(*ii*) by increasing the guide width a. Nevertheless, once a is bigger than

$$\left(\frac{R\lambda^2}{\pi n_1^2}\right)^{\frac{1}{3}},$$

(where λ is the free space wavelength), there is little reduction of the loss;

(*iii*) by choosing the height of the guide large enough to confine the fields as much as possible within the guide in the direction normal to the plane of curvature.

In general, the radiation losses are small if

$$R > \frac{24\pi^2 \mid \xi_3 \mid^3}{\lambda^2},$$

where ξ_3 is the length over which the field decays by $1/e$ in medium 3 (Fig. 2).

Thin ribbons of glass, surrounded by air and oriented as in Fig. 6c, operate better with the electric field perpendicular to the ribbon's plane. Choosing the thickness $a = 0.055\lambda$, the attenuation of the straight guide is 1 percent of the attenuation in glass, and the radius of curvature which doubles that low attenuation is $20{,}000\lambda$.

The dielectric guide for integrated optical circuitry seems suitable to negotiate bends and to make resonant loops of small radii of curvature and small radiation losses. For example, for

$$n_1 = 1.5$$

$$a = \frac{\lambda}{2n_1\left(1 - \frac{n_3^2}{n_1^2}\right)^{\frac{1}{2}}} \quad \text{(single mode guide)}$$

a 1 percent attenuation (0.087 dB) resulting from radiation in a length of guide equal to R is achieved with the following values

$1 - \frac{n_3}{n_1}$	$\frac{a}{\lambda}$	$\frac{R}{\lambda}$
0.1	0.745	30
0.01	2.36	1060
0.001	7.45	37000

The smaller $n_1 - n_3$, the larger the radius of curvature. For $\lambda = 0.63\mu$, if one wants to keep R below 1 mm, the difference between the internal and external refractive indices must be larger than 0.01.

Large cross section dielectric guides capable of supporting many modes are far more sensitive to mode conversions than to radiation losses. For the fundamental mode, the power conversion loss at the junction between a straight and a curved section of a multimode guide is

$$c^2 = \left(\pi n_1^2 \frac{a^3}{\lambda^2 R}\right)^2.$$

For $n_1 = 1.5$, $a = 6.3\mu$, and $\lambda = 0.63\mu$, the radius of curvature R that produces a power conversion c^2 of 0.01 is 45 mm. The radiation loss in a length of guide equal to R is many orders of magnitude below 0.01.

APPENDIX

Field Analysis of the Curved Guide

Figure 2 shows the geometry and dielectric distribution of the curved guide. In this appendix two families of modes are found, E^x_{pq} and E^y_{pq}; each is studied separately.

A.1 E^x_{pq} *Modes: Polarization Along* x

The field components in each region should be written as integral expressions, but, as discussed in Section II, the power propagating through the shaded areas is neglected, and the field matching is performed only along the sides of region 1. Consequently, those field components do not need to be so general. As a matter of fact, the simplest field components in the mth of the five areas are[16]

$$H_{xm} = \frac{1}{k_m^2 - k_{ym}^2} \frac{\partial^2 H_{ym}}{\partial x\, \partial y},$$

$$H_{ym} = e^{-i\nu\theta + i\omega t} \cdot \begin{cases} M_1 J_\nu[(k_1^2 - k_{y1}^2)^{\frac{1}{2}}(R + x) + \psi_1] \cos(k_{y1} y + \Omega_1) & \text{for } m = 1 \\ M_{2,4} J_\nu\left[\left[k_{2,4}^2 - k_{y2,4}^2\right]^{\frac{1}{2}}(R + x) + \psi_{2,4}\right] \exp\left[\mp i k_{y2,4} y\right] & \text{for } m = 2, 4 \\ M_3 H_\nu^{(2)}[(k_3^2 - k_{y3}^2)^{\frac{1}{2}}(R + x)] \cos(k_{y3} y + \Omega_3) & \text{for } m = 3 \\ M_5 J_\nu[(k_5^2 - k_{y5}^2)^{\frac{1}{2}}(R + x)] \cos(k_{y1} y + \Omega_5) & \text{for } m = 5 \end{cases},$$

$$H_{zm} = \frac{i}{k_m^2 - k_{ym}^2} \frac{\nu}{R + x} \frac{\partial H_{ym}}{\partial y},$$

$$E_{xm} = -\frac{\omega\mu}{k_m^2 - k_{ym}^2} \frac{\nu}{(R + x)} H_{ym},$$

$$E_{ym} = 0,$$

$$E_{zm} = \frac{-i\omega\mu}{k_m^2 - k_{ym}^2} \frac{\partial H_{ym}}{\partial x}, \tag{29}$$

in which M_m is the amplitude of the field in the mth medium; ψ_m and Ω_m are constants that locate the field maxima in region m; ω is the angular frequency; ϵn_m^2 and μ, the permittivity and permeability of each medium, are related by $k_m^2 = k^2 n_m^2 = \omega^2 \epsilon \mu n_m^2$; k_{ym} is the propagation constant along y in medium m; and J_ν and $H_\nu^{(2)}$ are Bessel and Hankel functions, respectively.

Strictly speaking, the H_y component in media 1, 2, and 4 should be written as a sum of Bessel functions of the first and second kind, but later on they are approximated by circular functions; therefore, we do not make any mistake using only the Bessel function of the first kind with an arbitrary phase constant in the argument.

We consider only guide geometries for which the guide wavelengths measured in the x and y directions in medium 1 are large compared with the wavelength measured in the z direction. This means that (*i*)

$$\frac{\partial H_{ym}}{\partial x} \ll \frac{\nu}{R}, \tag{30}$$

and, as a consequence, the field component H_{x1} is very small compared with H_z and is neglected; (*ii*) the propagating modes are basically of the TEM type.

In order to match the remaining components along the boundaries of medium 1, the field components in media 1, 2, and 4 must have the same dependence along x, while the field components in media 1, 3, and 5 must have the same dependence along y. Therefore

$$k_{y1} = k_{y3} = k_{y5} = k_y, \tag{31}$$

$$k_1^2 - k_y^2 = k_2^2 - k_{y2}^2 = k_4^2 - k_{y4}^2, \tag{32}$$

$$\psi_1 = \psi_2 = \psi_4 = \psi, \quad \text{and} \quad \Omega_1 = \Omega_3 = \Omega_5 = \Omega. \tag{33}$$

Furthermore, the field matching yields the following four equations from which two characteristic equations will be derived

$$\tan\left(k_y \frac{b}{2} + \Omega\right) = i \frac{k_{y2}}{k_y}, \qquad \tan\left(k_y \frac{b}{2} - \Omega\right) = i \frac{k_{y4}}{k_y} \tag{34}$$

$$\frac{J_\nu(\rho_{13})}{J'_\nu(\rho_{13})} = \frac{\rho_3}{\rho_{13}} \frac{H_\nu^{(2)}(\rho_3)}{H_\nu^{(2)\prime}(\rho_3)}, \quad \text{and} \quad \frac{J_\nu(\rho_{15})}{J'_\nu(\rho_{15})} = \frac{\rho_5}{\rho_{15}} \frac{J_\nu(\rho_5)}{J'_\nu(\rho_5)} \tag{35}$$

where

$$\left.\begin{aligned} \rho_{13} &= R(k_1^2 - k_y^2)^{\frac{1}{2}} + \psi, & \rho_{15} &= (R - a)(k_1^2 - k_y^2)^{\frac{1}{2}} + \psi \\ \rho_3 &= R(k_3^2 - k_y^2)^{\frac{1}{2}}, \quad \text{and} & \rho_5 &= (R - a)(k_5^2 - k_y^2)^{\frac{1}{2}}. \end{aligned}\right\} \tag{36}$$

Similar to what happens with the straight guide, equations (34) and (35) are the boundary conditions of two independent problems far simpler than the one depicted in Fig. 2. Thus, for a dielectric slab infinite in the x and z directions and with dimensions and refractive indices as depicted in Fig. 13a, the boundary conditions for modes with no E_y component coincide with equation (34). Similarly, for a bent slab infinite in the y direction as shown in Fig. 13b, the boundary conditions for modes with a negligible H_x component coincide with equation (35).

The elimination of Ω between the two expressions of equation (34) yields the characteristic equation for the plane slab[10]

$$k_y b = q\pi - \tan^{-1} \frac{1}{\left[\left(\frac{\pi}{A_2 k_y}\right)^2 - 1\right]^{\frac{1}{2}}} - \tan^{-1} \frac{1}{\left[\left(\frac{\pi}{A_4 k_y}\right)^2 - 1\right]^{\frac{1}{2}}}, \quad (37)$$

in which

$$A_{\substack{2\\4}} = \frac{\lambda}{2\left(n_1^2 - n_{\substack{2\\4}}^2\right)^{\frac{1}{2}}}; \quad (38)$$

the $\tan^{-1}$ functions are to be taken in the first quadrant, and the arbitrary integer q is the order of the mode, that is, the number of extrema of each field component within the guiding rod in the y direction.

The transcendental equation (37) has an approximate closed form solution already found in Ref. 10

$$k_y \cong \frac{q\pi}{b}\left(1 + \frac{A_2 + A_4}{\pi b} + \cdots\right)^{-1}, \quad (39)$$

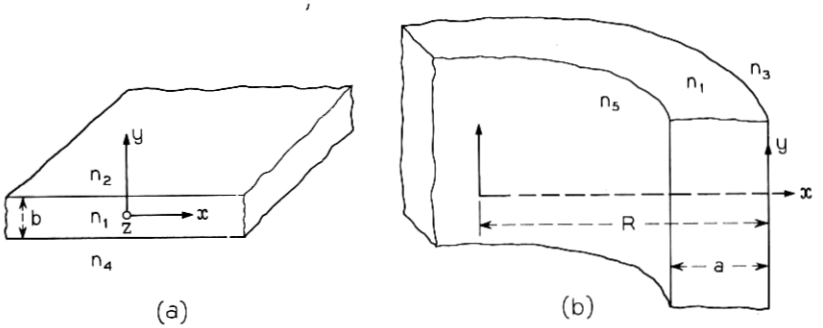

Fig. 13 — Guiding dielectric slabs.

which is valid only when b is so large that

$$\frac{A_2 + A_4}{\pi b} \ll 1 \tag{40}$$

and consequently the parenthesis is close to unity.

The field components in media 2 and 4 decay exponentially by $1/e$ in lengths η_2 and η_4, which are deduced from equation (32) to be

$$\eta_{\substack{2\\4}} = \frac{1}{\left| k_{y\substack{2\\4}} \right|} = \frac{1}{\left(k_1^2 - k_{\substack{2\\4}}^2 - k_y^2\right)^{\frac{1}{2}}}. \tag{41}$$

Let us consider the solution of the characteristic equation of the bent slab (Fig. 13b). For guided modes, both the arguments and the order of the Bessel and Hankel functions involved in equation (35) are large compared with unity, and consequently they can be replaced by their Watson's first term approximations,[17]

$$\left.\begin{aligned} J_\nu(\rho) &= \left[\frac{2}{\pi(\rho^2 - \nu^2)^{\frac{1}{2}}}\right]^{\frac{1}{2}} \begin{cases} \frac{1}{2}\exp\left[-\frac{(\nu^2 - \rho^2)^{\frac{3}{2}}}{3\nu^2}\right] & \text{for } \nu > \rho \\ \sin\left[\frac{(\rho^2 - \nu^2)^{\frac{3}{2}}}{3\nu^2} + \frac{\pi}{4}\right] & \text{for } \rho > \nu \end{cases} \\ Y_\nu(\rho) &= -\left[\frac{2}{\pi(\rho^2 - \nu^2)^{\frac{1}{2}}}\right]^{\frac{1}{2}} \begin{cases} \exp\left[\frac{(\nu^2 - \rho^2)^{\frac{3}{2}}}{3\nu^2}\right] & \text{for } \nu > \rho \\ \cos\left[\frac{(\rho^2 - \nu^2)^{\frac{3}{2}}}{3\nu^2} + \frac{\pi}{4}\right] & \text{for } \rho > \nu. \end{cases} \end{aligned}\right\} \tag{42}$$

These expressions are valid if

$$\frac{\nu^2}{(\rho^2 - \nu^2)^{\frac{3}{2}}} \ll 1. \tag{43}$$

Introducing these approximations for the Bessel functions in both equations (35) and eliminating ψ between them, we obtain the characteristic equation for the bent slab

$$\begin{aligned} &\frac{1}{3\nu^2}\left[(\rho_{13}^2 - \nu^2)^{\frac{3}{2}} - (\rho_{15}^2 - \nu^2)^{\frac{3}{2}}\right] \\ &\quad = p\pi - \tan^{-1}\left(\frac{n_3^2}{n_1^2}\left[\frac{\rho_{13}^2 - \nu^2}{\nu^2 - \rho_3^2}\right]^{\frac{1}{2}}\left\{1 + i\exp\left[-\frac{2}{3}\frac{(\nu^2 - \rho_3^2)^{\frac{3}{2}}}{\nu^2}\right]\right\}\right) \\ &\qquad - \tan^{-1}\frac{n_5^2}{n_1^2}\left(\frac{\rho_{15}^2 - \nu^2}{\nu^2 - \rho_5^2}\right)^{\frac{1}{2}}, \end{aligned} \tag{44}$$

in which p is an arbitrary integer bigger than zero which determines the order of the mode in the x direction, and the $\tan^{-1}$ functions are to be taken in the first quadrant.

Let us rewrite this equation substituting ρ_3, ρ_5, ρ_{13}, and ρ_{15} by the values given in equation (36); furthermore, let

$$A_{\substack{3\\5}} = \frac{\lambda}{2\left(n_1^2 - n_{\substack{3\\5}}^2\right)^{\frac{1}{2}}}, \tag{45}$$

$$\nu = k_z R \tag{46}$$

and

$$k_z = (k_1^2 - k_y^2 - k_x^2)^{\frac{1}{2}}. \tag{47}$$

Because of these two last definitions, k_z, k_x, and k_y are the axial and the transverse propagation constants at $x = 0$. The characteristic equation (44) then becomes

$$\begin{aligned}\frac{Rk_x^3}{3k_z^2}\left[1 - \left(1 - \frac{2ak_z^2}{k_x^2 R}\right)^{\frac{3}{2}}\right] &= p\pi - \tan^{-1}\frac{n_3^2}{n_1^2}\frac{1 + i\exp\left\{-\frac{2}{3}\frac{\pi^3 R}{k_x^2 A_3^3}\left[1 - \left(\frac{k_x A_3}{\pi}\right)^2\right]^{\frac{3}{2}}\right\}}{\left[\left(\frac{\pi}{k_x A_3}\right)^2 - 1\right]^{\frac{1}{2}}} \\ &\quad - \tan^{-1}\frac{n_5^2}{n_1^2}\left[\frac{\left[1 - \frac{a}{R}\right]^2(k_1^2 - k_y^2) - k_z^2}{k_z^2 - \left(1 - \frac{a}{R}\right)^2(k_5^2 - k_y^2)}\right]^{\frac{1}{2}}.\end{aligned} \tag{48}$$

To solve this equation for k_x we expand the left side and the second $\tan^{-1}$ in powers of $1/R$ and the first $\tan^{-1}$ in powers of the exponential. Assuming R is large and keeping the first term of each perturbation calculation, the solution of equation (48) is

$$k_x = k_{x0}\left(1 + \frac{2c}{ak_{x0}} - i\frac{k_{x0}\alpha_c}{k_{x0}^2}\right), \tag{49}$$

where

$$c = \frac{1}{2k_{x0}a}\left(\frac{\pi a}{A_3}\right)^3 \frac{1}{\Re}\frac{1 + 2F_5}{1 + F_3 + F_5} \tag{50}$$

and

$$\alpha_c = \frac{k_{x0}^2}{k_{z0}}\left[1 - \left(\frac{k_{x0}A_3}{\pi}\right)^2\right]F_3 \frac{\exp\left\{-\frac{\Re}{3}\left[1 - \left(\frac{k_{x0}A_3}{\pi}\right)^2\left(1 + \frac{2c}{ak_{x0}}\right)^2\right]^{\frac{3}{2}}\right\}}{1 + F_3 + F_5}, \tag{51}$$

in which

$$F_{\substack{3\\5}} = \left(\frac{n_{\substack{3\\5}}}{n_1}\right)^2 \frac{A_{\substack{3\\5}}}{\pi a\left[1 - \left(\frac{k_{x0}A_{\substack{3\\5}}}{\pi}\right)^2\right]^{\frac{1}{2}}} \frac{1}{1 - \left[1 - \frac{n_{\substack{3^2\\5^2}}}{n_1^2}\right]\left(\frac{k_{x0}A_{\substack{3\\5}}}{\pi}\right)^2}, \tag{52}$$

$$\Re = \frac{2\pi^3 R}{k_{x0}^2 A_3^3} = 2(n_1^2 - n_3^2)^{\frac{3}{2}} \frac{k^3 R}{k_{x0}^2}, \tag{53}$$

$$k_{z0} = (k_1^2 - k_y^2 - k_{x0}^2)^{\frac{1}{2}}, \tag{54}$$

and k_{x0} is the solution of the equation

$$k_{x0}a = p\pi - \tan^{-1}\frac{n_3^2}{n_1^2}\frac{1}{\left[\left(\frac{\pi}{k_{x0}A_3}\right)^2 - 1\right]^{\frac{1}{2}}} - \tan^{-1}\frac{n_5^2}{n_1^2}\frac{1}{\left[\left(\frac{\pi}{k_{x0}A_5}\right)^2 - 1\right]^{\frac{1}{2}}}. \tag{55}$$

This is the physical interpretation of equation (49): the transverse propagation constant k_x measured at $x = 0$ is made of three terms. The first term, k_{x0}, is the transverse propagation constant of the guide without curvature; the second and third terms are perturbations related to the change of field profile and radiation introduced by the curvature. It is easy to find that c^2 is the mode conversion loss that would exist at a junction between a straight guide and a curved one, and α_c is the attenuation coefficient of the curved guide.

The field components in media 3 and 5 decay almost exponentially away from the guide. The length ξ_3, over which the intensity in medium 3 decays by $1/e$, is derived as in equation (41) to be

$$\xi_3 = \frac{1}{|k_{x3}|} = \frac{1}{(k_1^2 - k_3^2 - |k_x^2|)^{\frac{1}{2}}} \tag{56}$$

and only approximately

$$\xi_5 = \frac{1}{|k_{x5}|} = \frac{1}{(k_1^2 - k_5^2 - |k_x^2|)^{\frac{1}{2}}}. \tag{57}$$

All these equations have been derived under the assumption that inequality (43) is satisfied; this means that the field configuration of the curved guide is very close to that of the straight guide. In other words, $c \ll 1$. For a given R, if one chooses the width a of the guide large enough, these inequalities are not satisfied, the previous results are no longer applicable, and a new solution is needed. We proceed to find it.

Let us assume as a limiting case that in Fig. 2

$$a = R. \tag{58}$$

The characteristic equation derived from the first equation of (35), making $\psi = 0$, is

$$\frac{(\rho_{13}^2 - \nu^2)^{\frac{3}{2}}}{3\nu^2} = (p - \tfrac{1}{4})\pi - \tan^{-1} \frac{n_3^2}{n_1^2} \cdot \left(\frac{\rho_{13}^2 - \nu^2}{\nu^2 - \rho_3^2}\right)^{\frac{1}{2}} \cdot \left\{1 + i \exp\left[-\frac{2}{3} \frac{(\nu^2 - \rho_3^2)^{\frac{3}{2}}}{\nu^2}\right]\right\}. \tag{59}$$

Following similar steps to those taken to solve equation (44), we substitute ρ_{13}, ρ_3, and ν by the values given in equations (36) and (46); we obtain

$$\frac{R(k_x')^3}{3(k_z')^2} = (p - \tfrac{1}{4})\pi - \tan^{-1} \frac{n_3^2}{n_1^2} \cdot \frac{1 + i \exp\left\{-\frac{2}{3} \frac{\pi^3 R}{(k_z')^2 A_3^3} \left[1 - \left(\frac{k_x' A_3}{\pi}\right)^2\right]^{\frac{3}{2}}\right\}}{\left[\left(\frac{\pi}{k_x' A_3}\right)^2 - 1\right]^{\frac{1}{2}}} \tag{60}$$

The primes distinguish the symbols from those used previously.

To solve this equation we notice that for small losses it must be that

$$\frac{k_x' A_3}{\pi} \ll 1. \tag{61}$$

Therefore, the $\tan^{-1}$ can be replaced by its argument and the approximate solution of equation (60) is

$$k_x' = k_{x0}' \left[1 - i \frac{k_{x0}' \alpha_c}{(k_{x0}')^2}\right], \tag{62}$$

where

$$\alpha_c = \frac{n_3^2}{n_1^2} \frac{k_{x0}'}{kR(n_1^2 - n_3^2)^{\frac{1}{2}}}$$

$$\cdot \exp\left(-\frac{\mathcal{R}'}{3}\left\{1-\left[\frac{6\pi(p-\frac{1}{4})}{\mathcal{R}'}\right]^{\frac{2}{3}}\left[1-\frac{2}{3}\frac{n_3^2}{n_1^2}\left(\frac{6}{\pi^2(p-\frac{1}{4})^2\mathcal{R}'}\right)^{\frac{1}{2}}\right]\right\}^{\frac{3}{2}}\right), \tag{63}$$

$$k'_{x0} = [k_1^2 - k_\nu^2 - (k'_{x0})^2]^{\frac{1}{2}}, \tag{64}$$

$$k'_{x0} = \frac{\pi}{A_3}\left[\frac{6\pi(p-\frac{1}{4})}{\mathcal{R}'}\right]^{\frac{1}{3}}\left\{1-\frac{1}{3}\frac{n_3^2}{n_1^2}\left[\frac{6}{\pi^2(p-\frac{1}{4})^2\mathcal{R}'}\right]^{\frac{1}{2}}\right\}, \tag{65}$$

and

$$\mathcal{R}' = \frac{2\pi^3 R}{(k'_{x0})^2 A_3^3} = 2(n_1^2 - n_3^2)^{\frac{3}{2}}\frac{k^3 R}{(k'_{x0})^2}. \tag{66}$$

The field components outside the guide decay to $1/e$ in a length

$$\xi'_3 = \frac{1}{|k'_{x3}|} = \frac{1}{[k_1^2 - k_3^2 - (k'_{x0})^2]^{\frac{1}{2}}}. \tag{67}$$

A.2 E^y_{pq} *Modes: Polarization Along y*

The field components and propagation constants can be derived from those in Section A.1 by changing E into H, μ into $-\epsilon$, and vice versa. Except for their polarizations, the E^x_{pq} and E^y_{pq} modes are very similar.

The formulas equivalent to equations (37) and (41) are

$$k''_\nu b = q\pi - \tan^{-1}\frac{n_2^2}{n_1^2}\frac{1}{\left[\left(\frac{\pi}{A_2 k''_\nu}\right)^2 - 1\right]^{\frac{1}{2}}} - \tan^{-1}\frac{n_4^2}{n_1^2}\frac{1}{\left[\left(\frac{\pi}{A_4 k''_\nu}\right)^2 - 1\right]^{\frac{1}{2}}} \tag{68}$$

$$\eta''_{\substack{2\\4}} = \frac{1}{|k''_{\substack{\nu 2\\4}}|}\quad\frac{1}{\left(k_1^2 - k_{\substack{2\\4}}^2 - (k''_\nu)^2\right)^{\frac{1}{2}}}. \tag{69}$$

The double prime distinguish these symbols from those used before.

The equivalent formula to any of those between equation (45) and (67) can be derived from that formula by substituting the ratio of refractive indexes by unity, but leaving the differences between squares of indexes unchanged. For example, the formula equivalent to equation (52) for E^y_{pq} modes is

$$F''_{\substack{3\\5}} = \frac{A_{\substack{3\\5}}}{\pi a\left[1-\left(\frac{k''_{x0}A_{\substack{3\\5}}}{\pi}\right)^2\right]^{\frac{1}{2}}}\frac{1}{1-\left[1-\frac{n_{\substack{3\\5}}^2}{n_1^2}\right]\left(\frac{k_{x0}A_{\substack{3\\5}}}{\pi}\right)^2}. \tag{70}$$

REFERENCES

1. Miller, S. E., U. S. Patent 3434774, applied for February 2, 1965 granted March 25, 1969.
2. Karbowiak, A. E., "New Type of Waveguide for Light and Infrared Waves," Elec. Letters, *1*, No. 2 (April 1965), p. 47.
3. Wolff, P. A., unpublished work.
4. Miller, S. E., "Integrated Optics: An Introduction," B.S.T.J., this issue, pp. 2059–2069.
5. Kaplan, R. A., "Optical Waveguide of Macroscopic Dimension in Single-Mode Operation," Proc. IEEE, *51*, No. 8 (August 1963), p. 1144.
6. Schineller, E. R., "Summary of the Development of Optical Waveguides and Components," Wheeler Laboratories, Report #1471, April 1967.
7. Kapany, N. S., *Fiber Optics,* New York: Academic Press, 1967.
8. Stratton, J. A., *Electromagnetic Theory,* New York: McGraw-Hill, 1941, pp. 524–527.
9. Snitzer, E., "Cylindrical Dielectric Waveguide Modes," J. Opt. Soc. Amer., *51*, No. 5 (May 1961), pp. 491–498.
10. Marcatili, E. A. J., "Dielectric Rectangular Waveguide and Directional Coupler for Integrated Optics," B.S.T.J., this issue, pp. 2071–2102.
11. Schlosser, W., and Unger, H. G., "Partially Filled Waveguides and Surface Waveguides of Rectangular Cross-Section," *Advances in Microwaves,* New York: Academic Press, 1966, pp. 319–387.
12. Bracey, M. F., Cullen, A. L., Gillespie, E. F. F., and Staniforth, J. A., "Surface-Wave Research in Sheffield," IRE Trans. Antennas and Propagation, *AP7* (December 1959), pp. S219–S225.
13. Goell, J. E., "A Circular-Harmonic Computer Analysis of Rectangular Dielectric Waveguides," B.S.T.J., this issue, pp. 2133–2160.
14. Jones, A. L., "Coupling of Optical Fibers and Scattering in Fibers," J. Opt. Soc. Amer., *55*, No. 3 (March 1965), pp. 261–271.
15. Marcatili, E. A. J., and Miller, S. E., "Improved Relations Describing Directional Control in Electromagnetic Wave Guidance," B.S.T.J., this issue, pp. 2161–2188.
16. Stratton, J. A., *Electromagnetic Theory,* New York: McGraw-Hill, 1941, pp. 361.
17. Magnus, W., Oberhettinger, F., and Soni, R. P., *Formulas and Theorems for the Special Functions of Mathematical Physics,* New York: Springer-Verlag, 1966, p. 144.